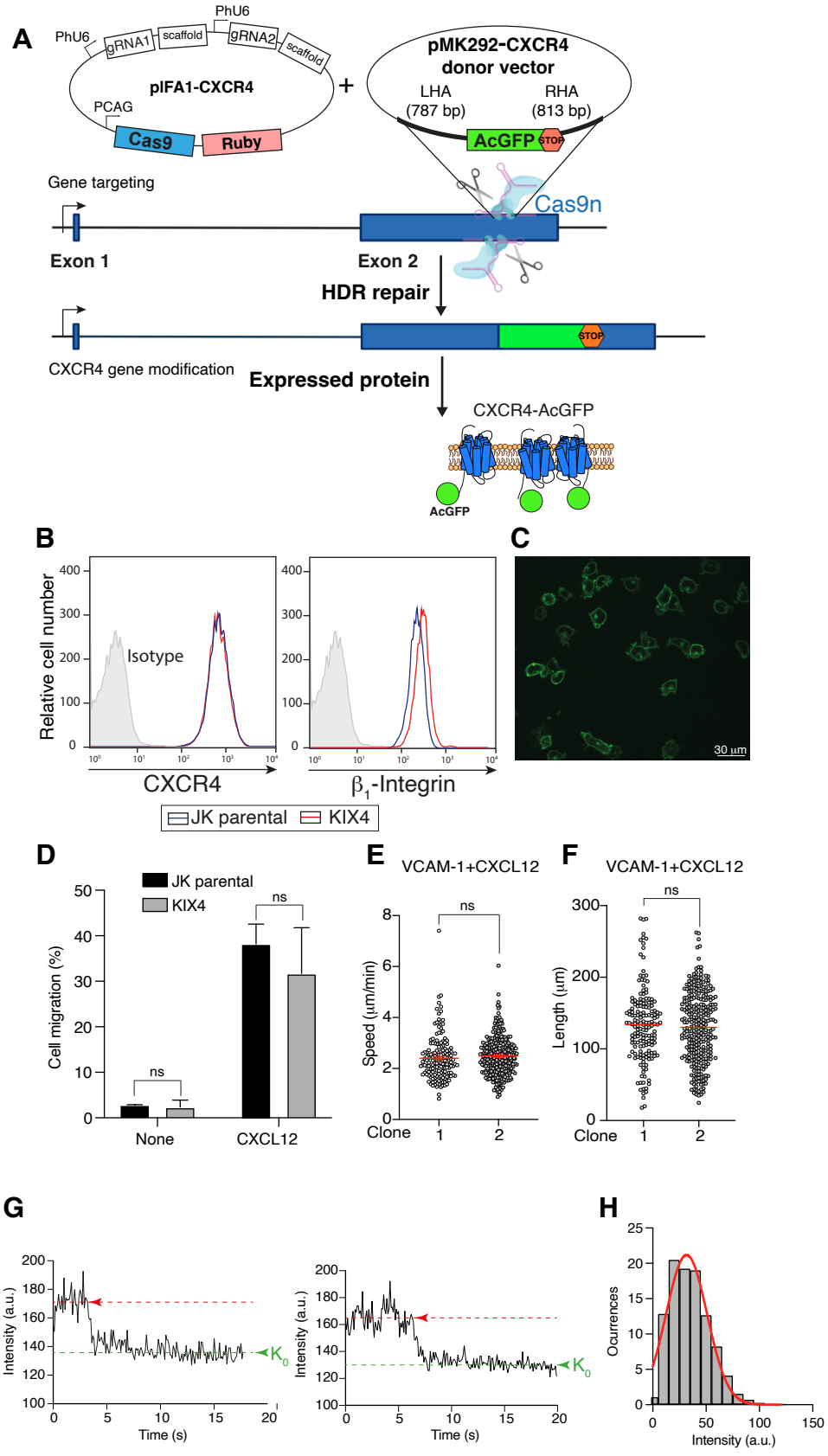

Supplementary Figure 1

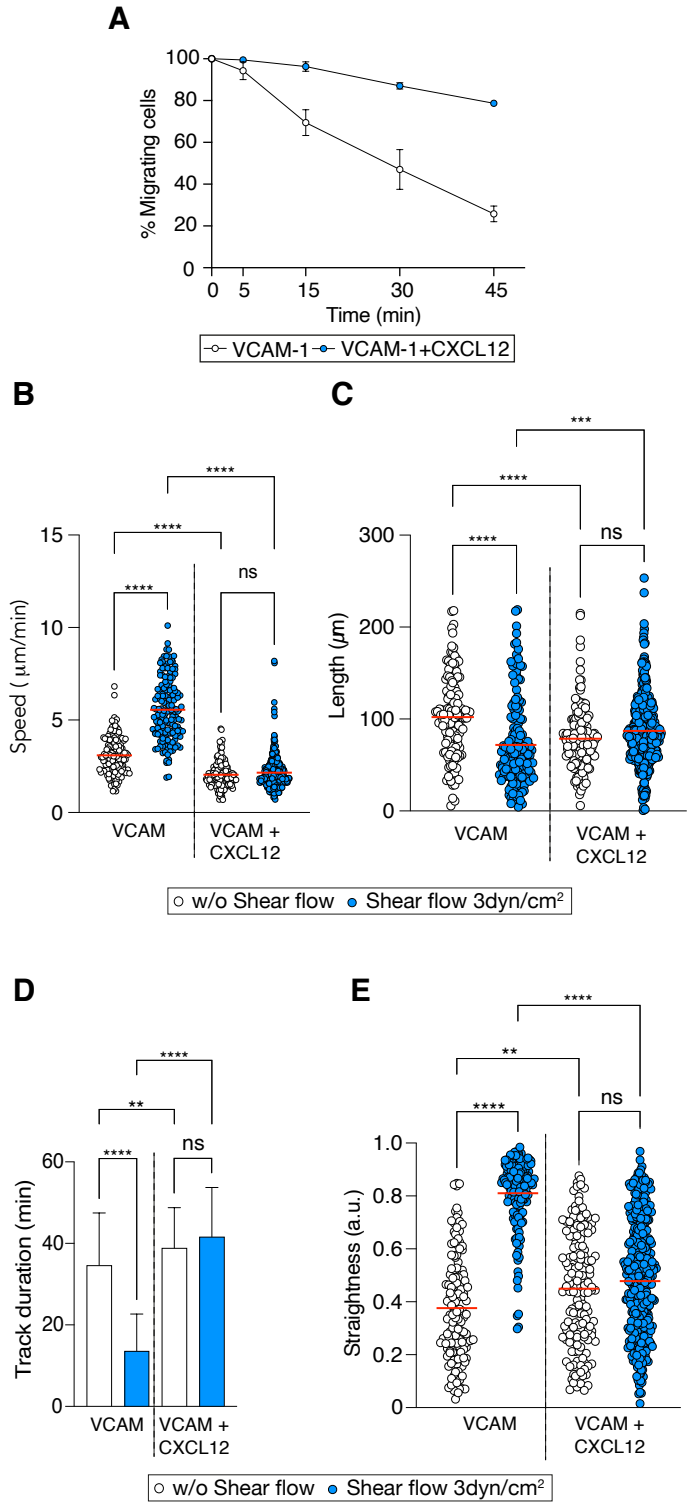

Supplementary Figure 2

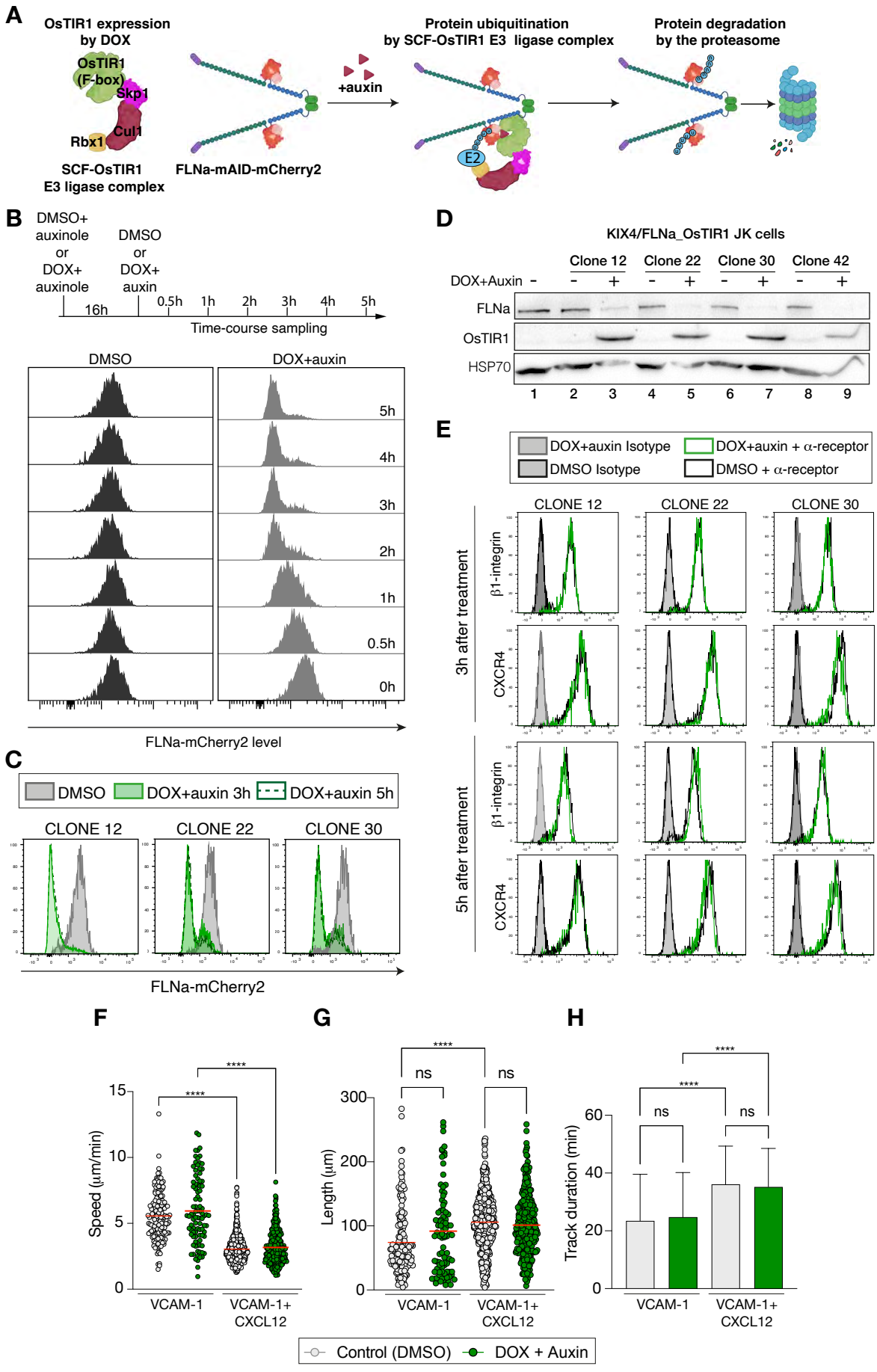

Supplementary Figure 3

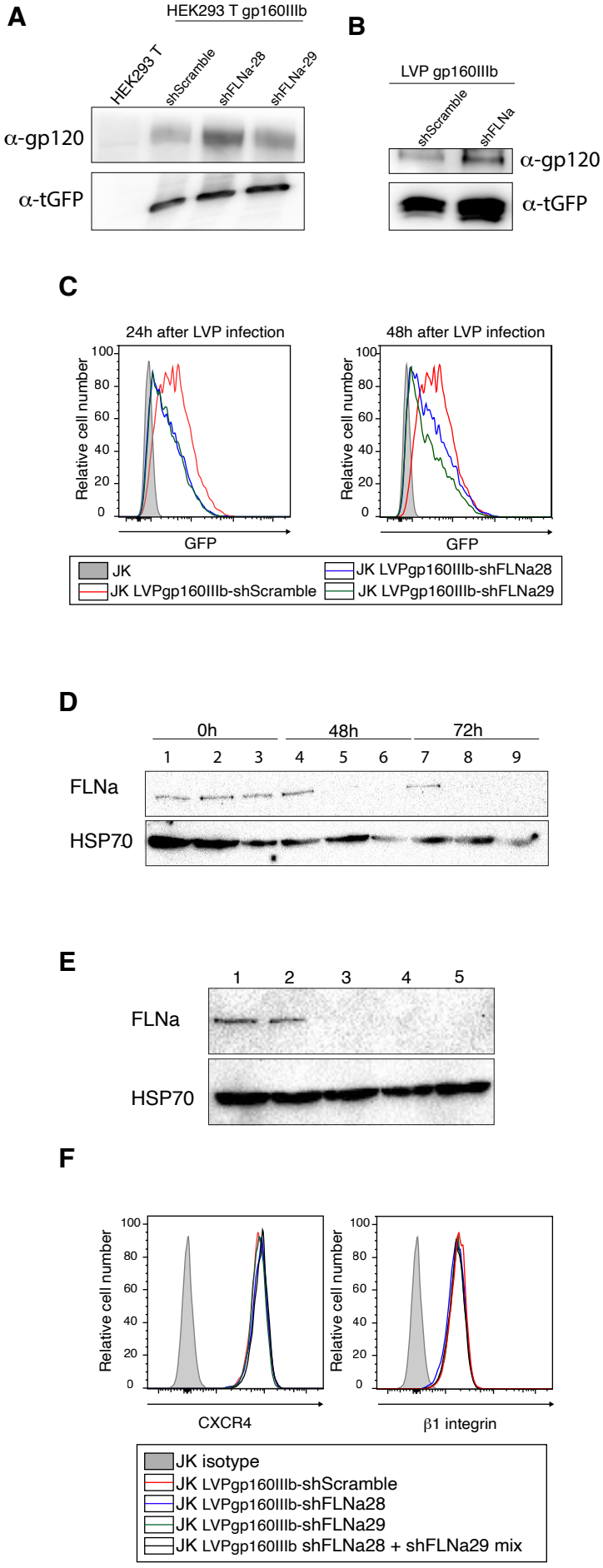

Supplementary Figure 4

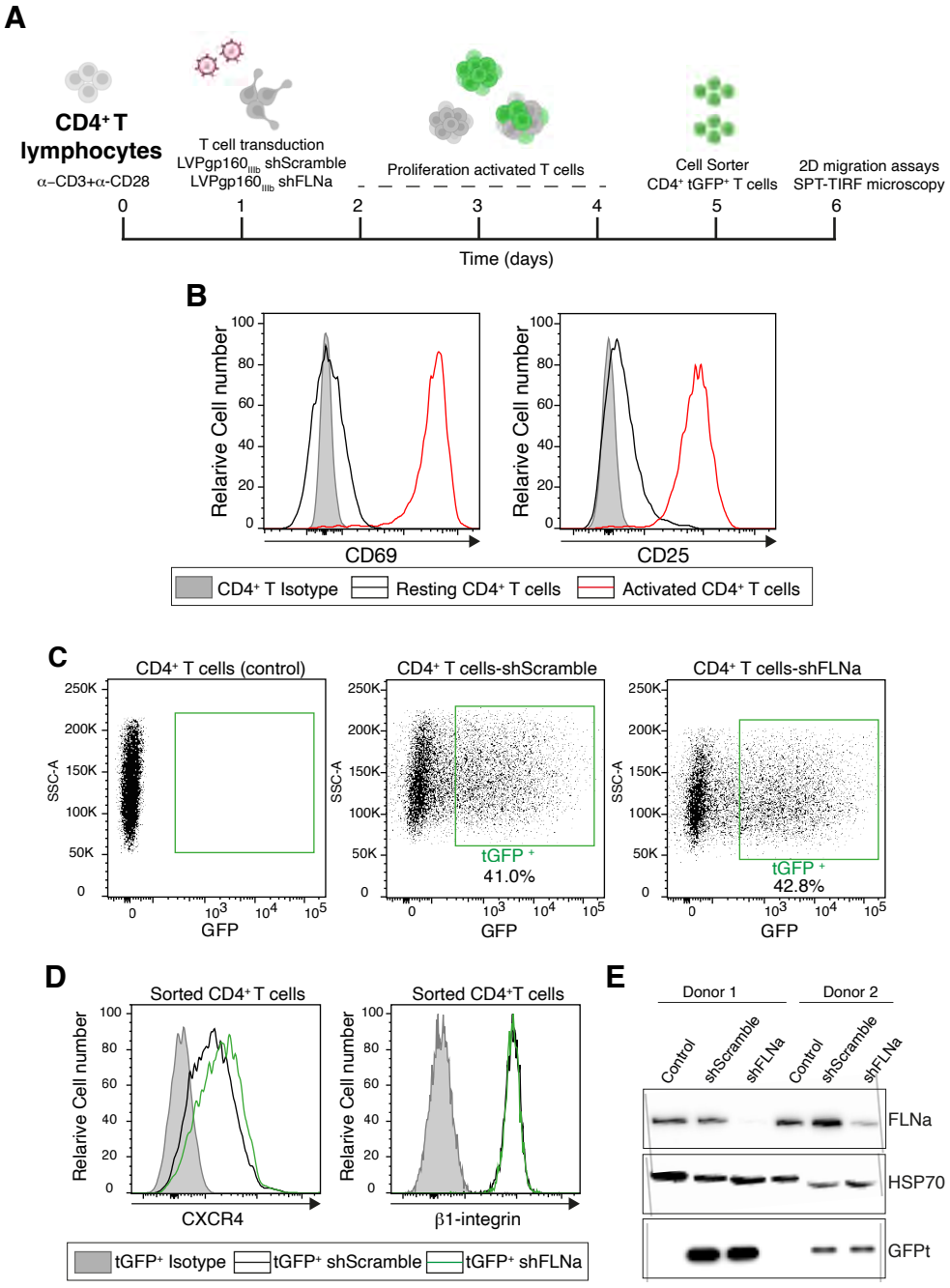

Supplementary Figure 5

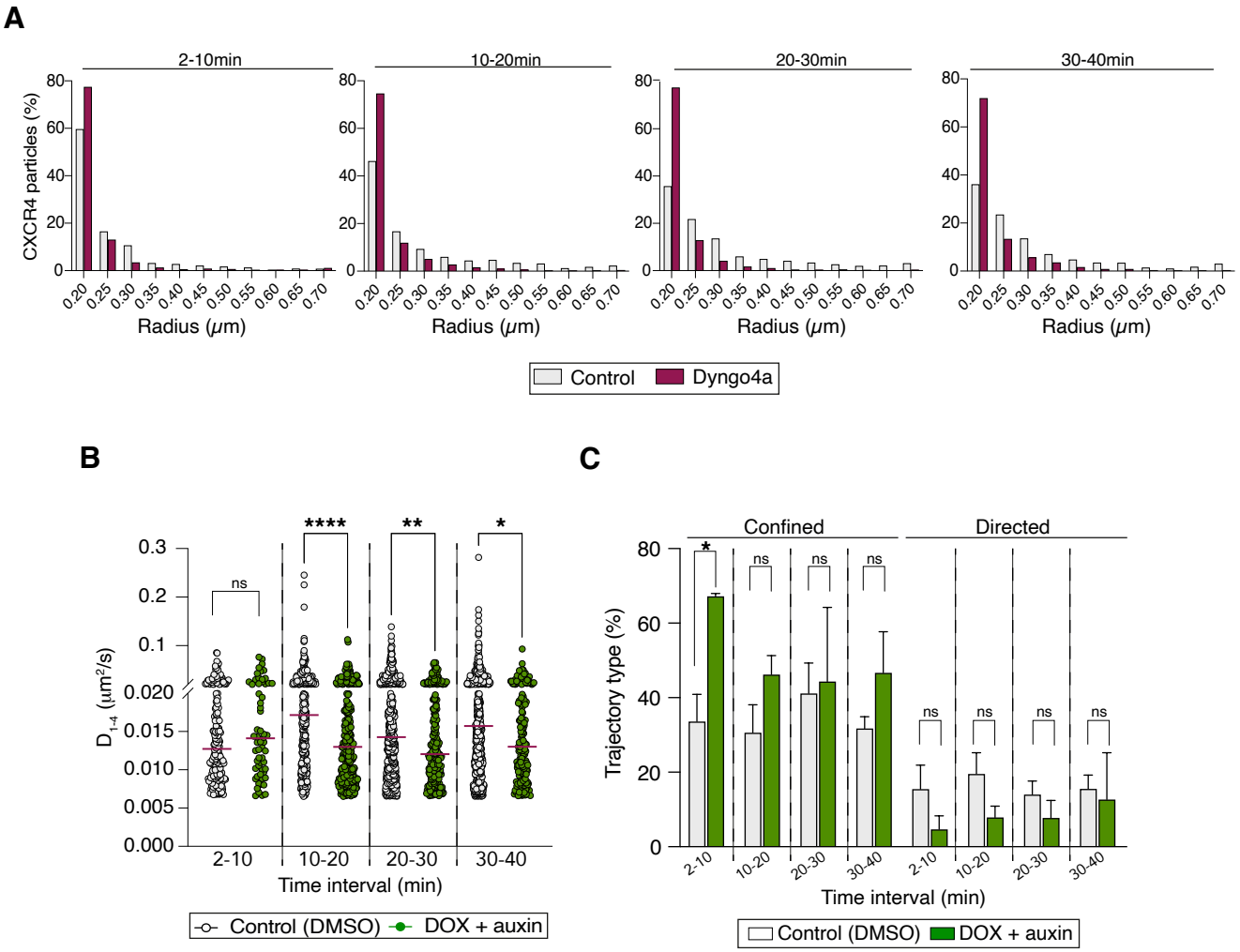

Supplementary FIGURE 6

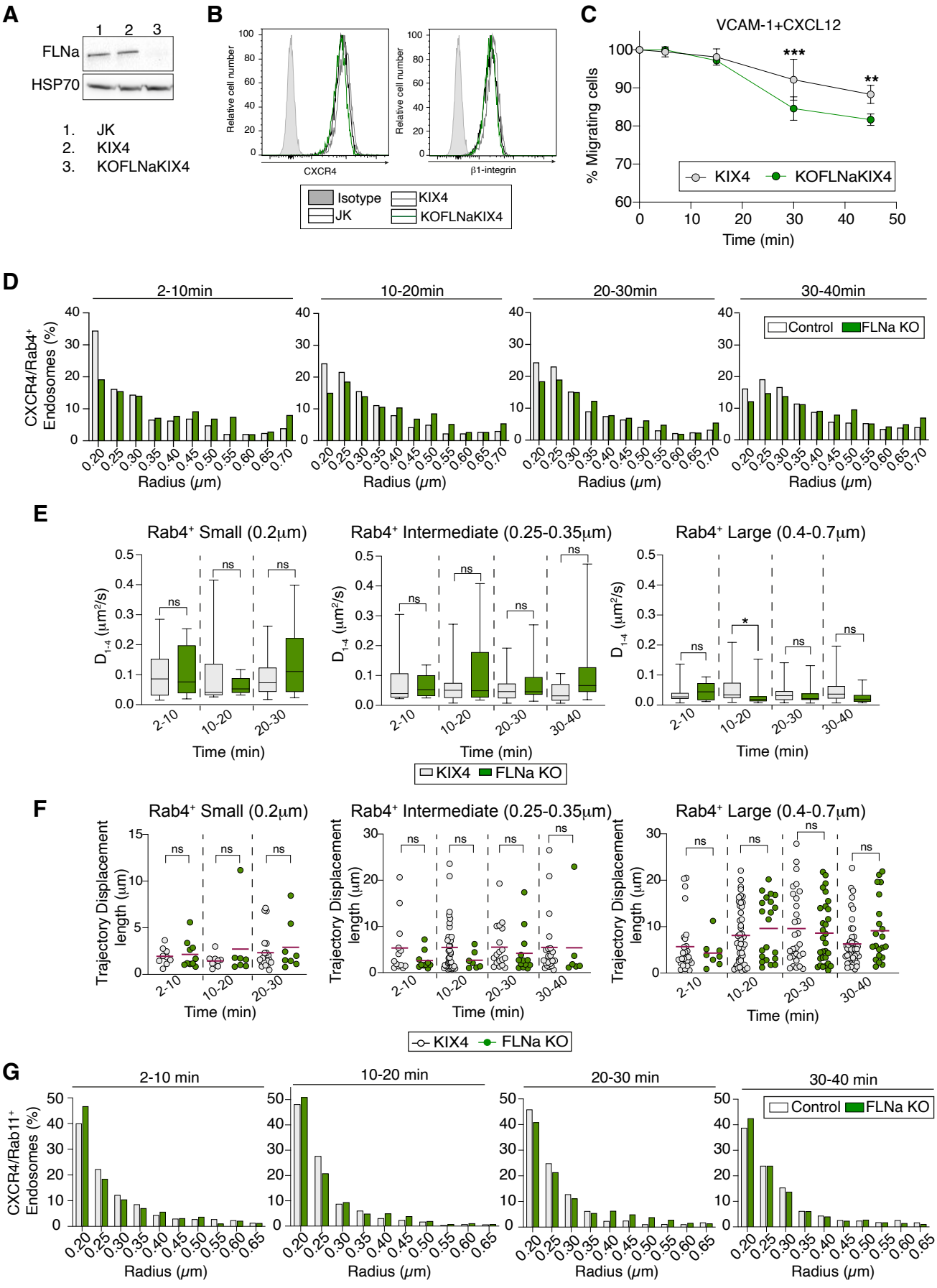

Supplementary FIGURE 7

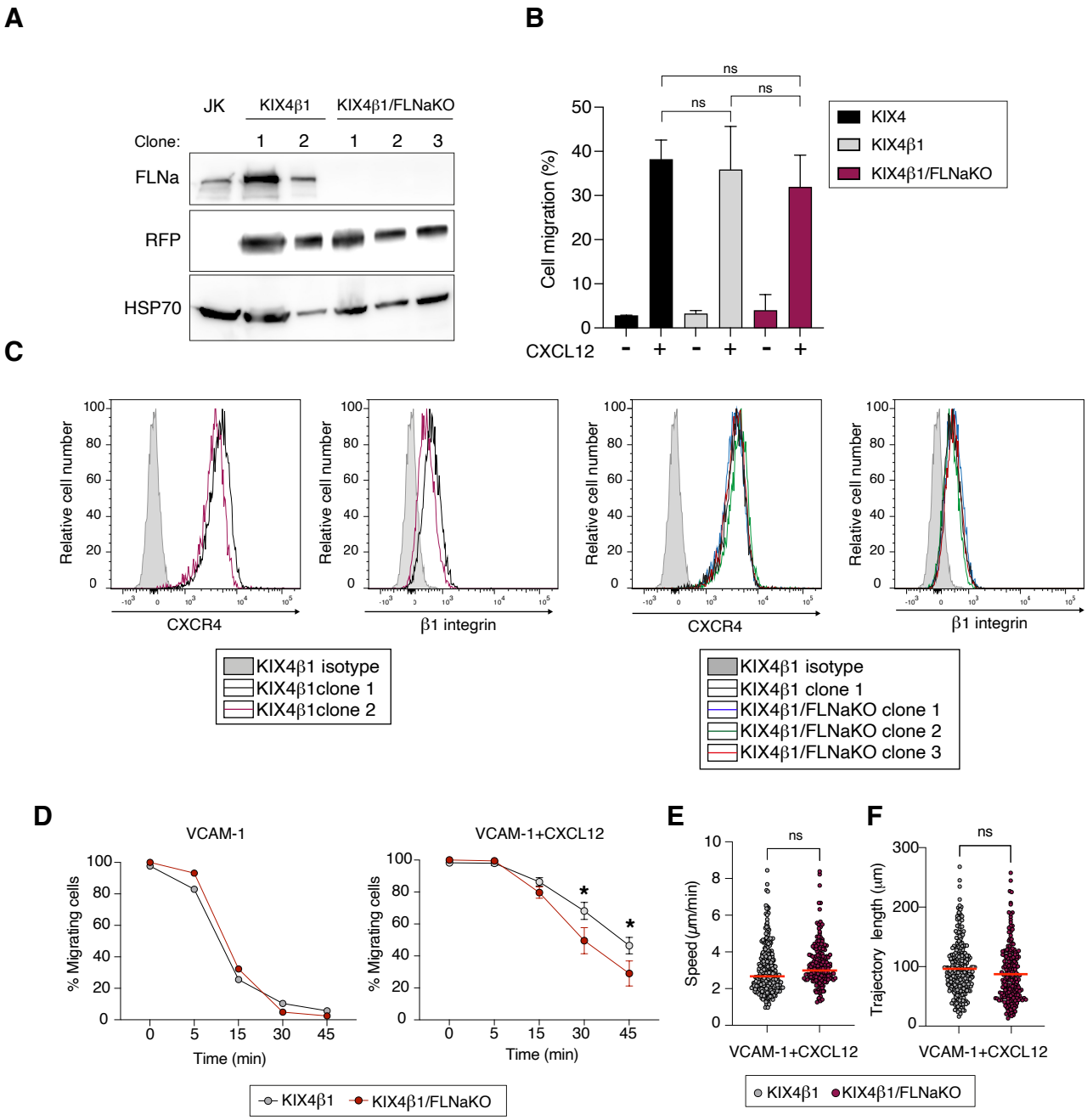

Supplementary FIGURE 8

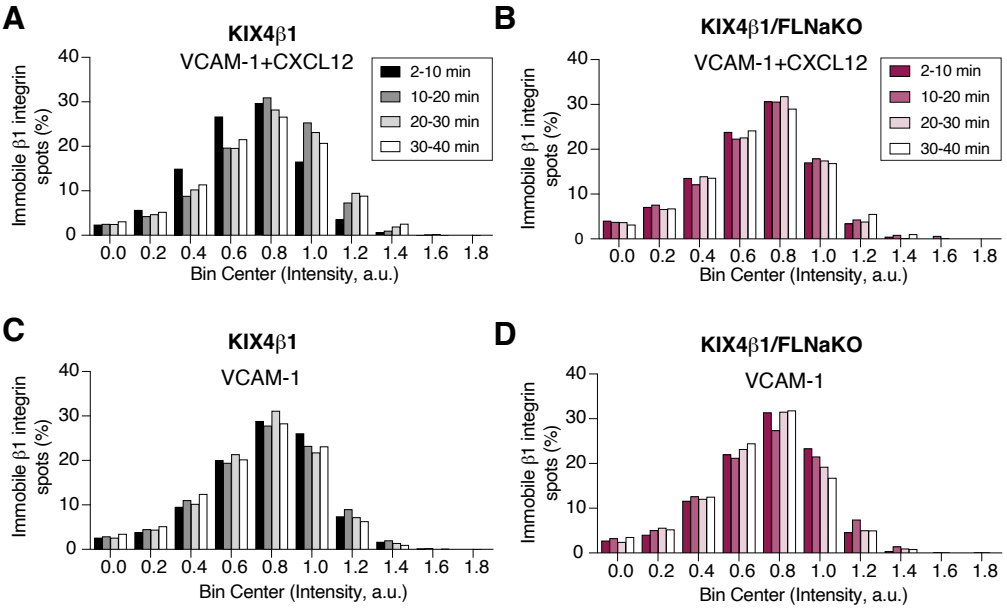

Supplementary FIGURE 9

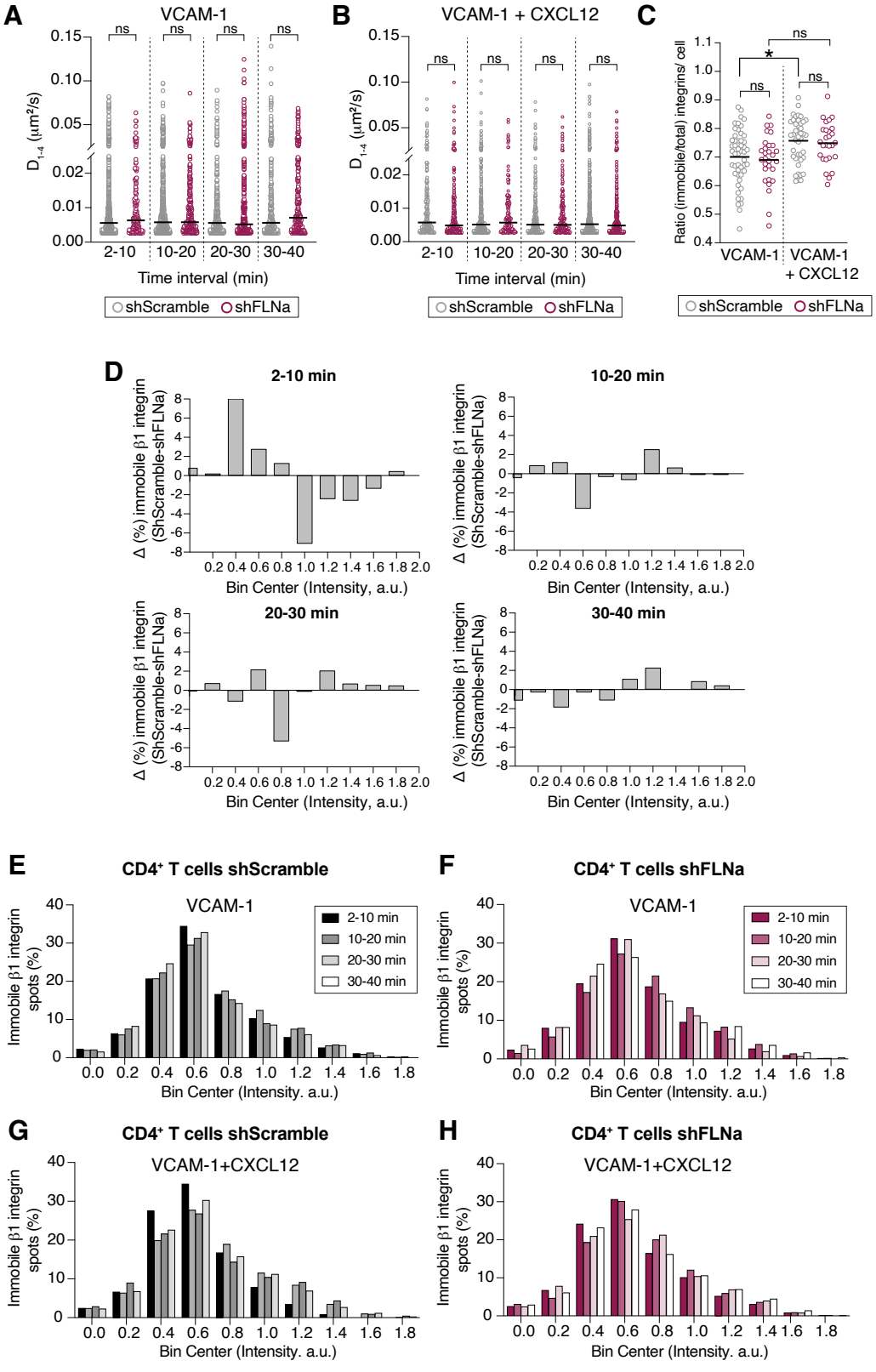

Supplementary FIGURE 10

Supplementary Figure 1. Generation and characterization of CXCR4-AcGFP knock-in JK cells, and determination of the monomeric AcGFP fluorescence intensity reference.

(A) Schematic representation of the CRISPRCas9n-mediated genome editing strategy used to generate CXCR4-AcGFP knock-in (KIX4) JK cells. The diagram shows the *CXCR4* locus and the vectors used (plFA1-CXCR4 and pMK292-CXCR4 donor vector). Cas9n-mediated genome editing introduces single-stranded DNA breaks, which are subsequently repaired preferentially by homology-directed repair (HDR). Two gRNAs are required to simultaneously cleave the antisense and sense strands, enhancing specificity and minimizing off-target cleavage. The plFA1 vector expresses Cas9n and either antisense or sense gRNAs targeting exon 2, together with a Ruby fluorescent marker, and is co-transfected with the pMK292 donor template containing AcGFP (with stop codon) flanked by left (LHA, 787bp) and right (RHA, 813 bp) homology arms. HDR-mediated repair results in site-specific insertion of AcGFP. See Methods for details.

(B) Representative flow cytometry analysis of parental JK and KIX4 cells using anti-CXCR4 (clone 447171) and anti-β1 integrin (TS2/16) antibodies (n=5).

(C) Representative confocal image showing CXCR4-AcGFP expression in migrating KIX4 cells on VCAM-1-coated µ-channel. Scale bar, 30 µm (see also Supplementaries Movies 1 and 2).

(D) Migration of parental JK and KIX4 cells in Boyden chambers in response to CXCL12 (20nM). Data are mean ± SD (n = 4). ns, not significant ($p \geq 0.05$).

(E-F) Migration speed (µm/s, E) and trajectory length (µm, F) of KIX4 clones migrating on VCAM-1+CXCL12-coated µ-channels. ns, $p \geq 0.05$. Related to Fig. 1A.

(G-H) Determination of reference fluorescence intensity of monomeric CD86–AcGFP expressed in JK cells by SPT-TIRF (related to Fig. 1F).

(G) Representative photobleaching steps from two individual CD86-AcGFP trajectories detected by SPT-TIRF. The background intensity (K_0), calculated from cellular background pixels and used for particle intensity correction, is shown as a reference.

(H) Fluorescence intensity histogram of monomeric CD86-AcGFP single particles, detected by one photobleaching step evaluation (164 trajectories from 51 cells in two independent experiments). The reference fluorescence intensity value for monomer (31.65 ± 19.22 a.u.) was obtained from the Gaussian fit (red line) of the histogram.

Supplementary Figure 2. Effects of shear flow on migrating KIX4 T cells (related to Fig. 2).

(A) Migration frequency of KIX4 cells in µ-channels coated with VCAM-1 alone or VCAM-1 plus CXCL12 under shear flow at different time points (mean ± SD, n = 3).

(B-E) Migration speed (µm/s, B), trajectory length (µm, C), track duration (min, D), and straightness (arbitrary units, E) of KIX4 T cells migrating in the conditions described in (A) with or without shear flow (w/o shear flow) on VCAM-1- or VCAM-1+CXCL12-coated µ-channels (mean, red line; ns, not significant, $p \geq 0.05$; *$p < 0.05$; **$p < 0.01$; ***$p < 0.001$; ****$p < 0.0001$). See also Supplementary Movies 5 and 6.

Supplementary Figure 3. Validation of FLNa depletion using the AID system and effects on KIX4/FLNa_OsTIR1 cell migration under shear flow.

(A) Schematic illustration of the auxin-inducible degron (AID) system. Upon DOX treatment, OsTIR1 is expressed and assembles with endogenous components to form the functional SCF-OsTIR1 E3 ubiquitin ligase complex in JK cells. In the presence of auxin, FLNa-mAID-mCherry2 is rapidly polyubiquitylated and subsequently degraded by the proteasome.

(B) Schematic timeline of cell treatments used for FLNa degradation and flow cytometry analysis.

(B–H) KIX4/FLNa_OsTIR1 JK cells were pretreated for 16h with DOX (2 µg/ml) and auxinole (400 µM), or with DMSO and auxinole (control), followed by medium replacement with fresh medium containing DOX (2 µg/ml) + auxin (500 µM) or DMSO (control) for the indicated timepoints.

(C) Representative flow cytometry analysis of FLNa-mAID-mCherry2 expression in different KIX4/FLNa_OsTIR1 JK cell clones treated with DMSO (control) or with DOX+auxin for 3h or 5h.

(D) Western blot analysis of FLNa and OsTIR1 expression in different KIX4/FLNa_OsTIR1 JK cell clones treated with DMSO (control) or with DOX+auxin for 3h. HSP70 was used as a loading control (n = 4).

(E) Representative flow cytometry analysis of surface CXCR4 and β1 integrin levels using specific antibodies (anti-CXCR4, clone 447171; anti-β1integrin, clone TS2/16) in

KIX4/FLNa_OsTIR1 JK cell clones treated with DMSO (control) or DOX+auxin for 3h or 5h (n = 5).

(F-H) Migration parameters of KIX4/FLNa_OsTIR1 JK cells under shear flow: (F) migration speed (µm/s), (G) trajectory length (µm) and (H) track duration (min). Cells were treated with DMSO (control) or DOX+auxin and analyzed in VCAM-1- and VCAM-1+CXCL12-coated µ-channels (mean, red line; ns, not significant, $p \geq 0.05$; *$p < 0.05$; ***$p < 0.001$; ****$p < 0.0001$). See also Supplementary Movies 7-10.

Supplementary Figure 4. Validation of FLNa depletion in JK cells using lentiviral particles carrying shRNA vectors.

(A) Lentiviral particles (LVPs) were generated by transient transfection of HEK 293T cells with pHXB2-env, psPAX2, and either pLKO.1-puro-CMV-TurboGFP carrying a scramble sh RNA (shScramble) or FLNa-trageting shRNA (shFLNa-28 or shFLNa-29). Expression of envelope and reporter proteins in packaging cells were confirmed by Western blot using anti-gp120 and anti-tGFP antibodies.

(B) Western blot analysis of LVP extracts carrying $gp160_{IIIb}$-shScramble or $gp160_{IIIb}$-shFLNa using anti-gp120 and anti-tGFP antibodies.

(C) Flow cytometry analysis of tGFP levels in JK cells infected with LVP$gp160_{IIIb}$-shScramble, LVP$gp160_{IIIb}$-shFLNa-28 or LVP$gp160_{IIIb}$-shFLNa-29 at 24h and 48h post-infection.

(D) Western blot analysis of FLNa expression in JK cells infected with LVP$gp160_{IIIb}$-shScramble (lanes 1, 4, 7), LVP$gp160_{IIIb}$-shFLNa-28 (lanes 2, 5, 8), or LVP$gp160_{IIIb}$-shFLNa-29 (lanes 3, 6, 9), at 0 h, 48 h, and 72 h post-infection. HSP70 was used as loading control.

(E) Western blot analysis of FLNa expression at 48 h post-infection in JK cells infected with LVP$gp160_{IIIb}$-shScramble (lane 2), LVP$gp160_{IIIb}$-shFLNa-28 (lane 3), LVP$gp160_{IIIb}$-shFLNa-29 (lane 4), or a combination of LVP$gp160_{IIIb}$-shFLNa-28 and LVP$gp160_{IIIb}$-shFLNa-29 (lane 5). Uninfected parental JK cells were included as control (lane 1). HSP70 was used as loading control.

(F) Flow cytometry analysis of plasma membrane CXCR4 and β1 integrin levels in JK cells infected with LVP$gp160_{IIIb}$-shScramble, LVP$gp160_{IIIb}$-shFLNa-28 or LVP$gp160_{IIIb}$-shFLNa-29 or the combination of LVP$gp160_{IIIb}$-shFLNA-28 and LVP$gp160_{IIIb}$-shFLNa-29 at 48h post-infection.

Supplementary Figure 5. Efficient FLNa knockdown in primary human CD4$^+$ T lymphocytes using lentiviral shRNA vectors: validation by flow cytometry and immunoblotting.

(A) Schematic overview of the experimental workflow for FLNa depletion in primary human CD4$^+$ T lymphocytes. Purified CD4$^+$ T cells from peripheral blood were activated with anti-CD3 and anti-CD28 Dynabeads. At 24h post-activation (Day 1), cells were transduced with LVPgp160$_{IIIb}$-shScramble or LVPgp160$_{IIIb}$-shFLNa. At 3 days post-infection (Day 5), tGFP$^+$ cells were sorted and culture for an additional 24 h prior to 2D migration assays under shear flow and SPT-TIRF microscopy (Day 6).

(B) Flow cytometry analysis of membrane CD69 and CD25 expression in resting (Day 0) and activated (Day 1) CD4$^+$ T lymphocytes (n = 4).

(C) Representative FACS plots of tGFP$^+$ CD4$^+$ T lymphocytes at Day 5. CD4$^+$ T cells–shScramble (middle panel) and CD4$^+$ T cells–shFLNa (right panel) correspond to cells transduced with LVPgp160IIIb-shScramble or LVPgp160IIIb-shFLNa, respectively. tGFP$^+$ populations were gated and sorted (green square). Activated, uninfected CD4$^+$ T cells were used as a control for gating (left panel).

(D) Flow cytometry analysis of plasma membrane CXCR4 and β1 integrin levels in sorted tGFP$^+$ CD4$^+$ T cells transduced with either LVPgp160$_{IIIb}$-shScramble (tGFP$^+$ shScramble) or LVPgp160 $_{IIIb}$-shFLNa (tGFP$^+$ shFLNa) (Day 5).

(E) Western blot analysis of FLNa and tGFP expression in sorted tGFP$^+$ CD4$^+$ T lymphocytes transduced with LVPgp160$_{IIIb}$-shScramble (shScramble) or LVPgp160 $_{IIIb}$-shFLNa (shFLNa) at Day 5. Uninfected, activated CD4$^+$ T lymphocytes were included as controls. HSP70 was used as a loading control. Samples from two independent donors (Donor 1 and Donor 2) are shown.

Supplementary Figure 6. FLNa-deficient T cells show reduced motility of large intracellular CXCR4 spots during CXCL12-mediated migration.

(A) KIX4 cells treated with Dyngo4a (dynamin inhibitor) or DMSO (control) were injected into VCAM-1 + CXCL12-coated μ-channels. Individual CXCR4 particle dynamics were analyzed at indicated migration intervals using SPT-TIRF microscopy with a 150 nm evanescent wave penetration. Frequency distribution of CXCR4 particle radii (μm) in control and Dyngo4a-treated KIX4 cells at 2-10, 10-20, 20-30 and 30-40 min after the onset of migration (control: 3320, 2723, 3455, 2788 trajectories in 22, 20,

23 and 21 cells respectively; Dyngo4a: 5383, 2471, 2049, 3553 trajectories in 31, 22, 13 and 24 cells, respectively; n = 3).

(B) Surface CXCR4 expression in KIX4 cells treated with Dyngo4a (100 μM, 30 min) or DMSO after 30 min of migration on VCAM-1+CXCL12-coated surfaces, analyzed by flow cytometry (mean ± SD, n = 3)

(C-D) Analysis of instantaneous diffusion coefficients ($\mu m^2/s$; C) and the proportion of trajectory types (%; D) of individual large CXCR4 endosomes (radius ≥0.4–0.7 μm) in KIX4/FLNa_OsTIR1 cells treated with DMSO (control) or DOX+auxin (FLNa-deficient). Cells were injected into VCAM-1+CXCL12-coated μ-channels and imaged using TIRF microscopy (150 nm evanescent wave penetration). Control: 212, 364 ,634 and 669 trajectories at 2-10, 10-20, 20-30, and 30-40 min, respectively; FLNa- deficient (DOX+auxin): 62, 338 ,233 and 179 trajectories for the same time intervals. Medians are shown in red (C); mean ± SD (D); n = 3; ns, $p \geq 0.05$; *$p < 0.05$, **$p < 0.01$, ****$p < 0.0001$).

Supplementary Figure 7. Functional characterization of KOFLNaKIX4 cells and extended analysis of CXCR4$^+$/Rab4$^+$ and CXCR4$^+$/Rab11$^+$ endosomes during migration.

(A) Western blot analysis of FLNa expression in parental JK (line 1), KIX4 (line 2) and KOFLNaKIX4 (line 3) cells. HSP70 was used as a loading control (n = 4).

(B) Representative flow cytometry analysis of surface CXCR4 (clone 447171) and β1 integrin (TS2/16) expression in parental JK, KIX4 and KOFLNaKIX4 cells (n = 3).

(C) Percentage of migrating KIX4 and KOFLNaKIX4 cells in μ-channels coated with VCAM-1 + CXCL12 under shear flow (3dyn/cm^2) (mean ± SD, n = 3; **$p < 0.01$, ***$p < 0.001$).

(D-F) KIX4 (control) and KOFLNaKIX4 (FLNa KO) cells were transiently transfected with mRuby-Rab4a. CXCR4$^+$/Rab4$^+$ cells were sorted and injected into VCAM-1+CXCL12 coated μ-channels. Fast recycling of CXCR4 was analyzed using dual-color SPT-TIRF microscopy.

(D) Frequency distribution of CXCR4$^+$/Rab4$^+$ endosome radii (μm) in control and FLNa KO cells at the indicated migration intervals (2-10, 10-20, 20-30 and 30-40 min; n = 4; Control: 339, 681, 485 and 666 trajectories in 29, 45, 37 and 45 cells, respectively; FLNa

KO: 366, 499, 774 and 448 trajectories in 31, 45, 46 and 41 cells, respectively). Related to Figure 5.

(E) D_{1-4} and (F) displacement lengths (µm) of individual small (left, ≤0.2 µm), intermediate (middle, 0.25-0.35 µm) and large (right, 0.4-0.7 µm) $CXCR4^+/Rab4^+$ endosome trajectories exhibiting directed motion at different migration intervals (n = 4; ns, $p \geq 0.05$; *$p < 0.05$). See also Figure 5.

(G) KIX4 (control) and KOFLNaKIX4 (FLNa KO) cells were transiently transfected with miRFP670_2-Rab11a. $CXCR4^+/Rab11^+$ cells were sorted and injected into VCAM-1+CXCL12 coated µ-channels. CXCR4 slow recycling was analyzed using dual-color SPT-TIRF microscopy. Frequency distribution of $CXCR4^+/Rab11^+$ endosome radii (µm) in control and FLNa KO cells at 2-10, 10-20, 20-30 and 30-40 min after migration onset. (control: 541, 947, 867 and 1115 trajectories in 45, 51, 44 and 51 cells, respectively; FLNa KO: 995, 1069, 983 and 1357 trajectories in 45, 46, 48 and 51 cells, respectively; n = 3;). Related to Figure 6.

Supplementary Figure 8. Functional characterization of KIX4β1 and KIX4β1 FLNa-deficient (KIX4β1/FLNaKO) cells.

(A) Immunoblot analysis of β1-integrin-mCherry2 (α-RFP) and FLNa expression in different clones of KIX4β1 and KIX4β1 FLNa-deficient (KIX4β1/FLNaKO) JK cells. JK parental cells were included as control. HSP70 was used as a loading control.

(B) Migration of KIX4, KIX4β1 and KIX4β1/FLNaKO JK cells in Boyden chambers in response to CXCL12 (20nM). Data are presented as mean ± SD (n = 4; ns, $p \geq 0.05$).

(C) Representative flow cytometry analysis of surface expression of CXCR4 (clone 447171) and β1 integrin (TS2/16) in KIX4β1 and KIX4β1/FLNaKO JK T cell clones (n = 4).

(D) Frequency of migrating KIX4β1 and KIX4β1/FLNaKO cells in µ-channels coated with either VCAM-1 alone (left) or VCAM-1 + CXCL12 (right), under shear flow (3 dyn/cm^2) (mean ± SD, n = 4; *$p < 0.05$). See also Supplementary Movies 22 and 23.

(E-F) Migration parameters of KIX4β1 and KIX4β1/FLNaKO cells in µ-channels coated with VCAM-1+CXCL12 under shear flow: (E) migration speed (µm/s) and (F) trajectory length (µm). Red line indicates the mean (ns, $p \geq 0.05$). See also Supplementary Movie 23.

Supplementary Figure 9. SPT analysis of immobile β1 integrin organization during T cell migration.

(A-D) SPT analysis of β1 integrin organization in KIX4β1 (A, C) and FLNa-deficient (KIX4β1/FLNaKO; B, D) T cells migrating on VCAM-1 or VCAM-1+CXCL12-coated μ-channels under shear flow.

Time-resolved frequency distribution of individual immobile β1 integrin spots according to fluorescence intensity bin centers (a.u.) in KIX4β1 and KIX4β1/FLNaKO cells migrating on VCAM-1+CXCL12 (A, B) or VCAM-1 alone (C, D) under shear flow. Data are shown for four migration time intervals: 2-10, 10-20, 20-30, and 30-40 minutes.

Supplementary Figure 10. Functional analysis of immoible β1 integrin dynamics and nanoscale organization during CXCL12-driven primary CD4$^+$ T cell migration under shear flow.

(A-B) $D_{1\text{-}4}$ distribution of individual β1 integrin trajectories in activated primary CD4$^+$ T lymphocytes infected with control LVPs $gp160_{IIIb}$-sh-Scramble (shScramble) or LVPs $gp160_{IIIb}$-sh-FLNa (shFLNa), migrating on VCAM-1 (A) or VCAM-1+CXCL12 (B) under shear flow at the indicated time intervals (median, black line; VCAM-1, shScramble: 15 cells (2-10 min, 646 trajectories), 15 (10-20 min, 777), 9 (20-30 min, 345), 15 (30-40 min, 337); shFLNa: 8 cells (2-10 min, 158), 6 (10-20 min, 332), 10 (20-30 min, 426), 7 (30-40 min, 305); VCAM-1+CXCL12, shScramble: 5 cells (2-10 min, 253), 11 (10-20 min, 465), 8 (20-30 min, 303), 21 (30-40 min, 710); shFLNa: 7 cells (2-10 min, 249), 4 (10-20 min, 150), 7 (20-30 min, 220) and 9 (30-40 min, 300); n = 3; ns, $p \geq 0.05$).

(C) Ratio of immobile to total β1 integrin spots per cell in activated primary CD4$^+$ T lymphocytes migrating on VCAM-1 or VCAM-1+CXCL12-coated μ-channels. Each dot represents the value from a single cell (n = 3; ns, $p \geq 0.05$; *$p < 0.05$).

(D) Time-resolved frequency distribution of individual immobile β1 integrin spots according to fluorescence intensity bin centers (arbitrary units, a.u.). Shown is the percentage difference (Δ %) in the proportion of β1 integrin spots within each fluorescence intensity bin between LVPs-shScramble and LVPs-shFLNa-transduced CD4$^+$ T lymphocytes migrating on VCAM-1+CXCL12 under shear flow (shScramble - shFLNa). Data are shown for four migration time intervals: 2-10, 10-20, 20-30, and 30-40 min (n = 3 independent experiments).

(E-H) Frequency distribution of individual immobile β1 integrin spots according to fluorescence intensity bin centers (arbitrary units, a.u.) in $CD4^+$ T lymphocytes transduced with LVPs-shScramble (E, G) or LVPs-shFLNa (F, H), migrating on VCAM-1 or VCAM-1+CXCL12 under shear flow at 2-10, 10-20, 20-30 and 30-40 min (VCAM-1, shScramble: 822 spots in 50 cells; shFLNa: 483 spots in 29 cells; VCAM-1+CXCL12, shScramble: 4778 spots in 42 cells; shFLNa: 2820 spots in 27 cells; n = 3). See Methods and Supplementary Movies 28-31.

Supplementary Movie 1. Related to Figure 1 and Supplementary Figure 1. Representative movie of KIX4 cell migration on VCAM-1-coated μ-channels. Fluorescence and DIC images are shown, covering the duration of cell migration, and the movie is displayed at 10 frames/second. Scale bar, 30 μm.

Supplementary Movie 2. Related to Figure 1 and Supplementary Figure 1. Representative movie of KIX4 cell migration on VCAM-1 and CXCL12-coated μ-channels. Fluorescence and DIC images are shown, covering the duration of cell migration, and the movie is displayed at 10 frames/second. Scale bar, 30 μm.

Supplementary Movie 3. Related to Figure 1. Representative movie of migrating KIX4 T cells captured by SPT-TIRF microscopy. Cells were injected into μ-channels coated with VCAM-1. The movie shows lateral diffusion of CXCR4 particles (mostly monomers) at various times points during cell migration. Time points are indicated in white in the upper left corner. The movie was acquired and displayed at 10 frames/s. Scale bar, 5 μm.

Supplementary Movie 4. Related to Figure 1. Representative movie of migrating KIX4 T cells captured by SPT-TIRF microscopy. Cells were injected into μ-channels coated with VCAM-1 and CXCL12. The movie shows lateral diffusion of CXCR4 particles (monomers, dimers and nanoclusters) at various times points during cell migration. Time points are indicated in white in the upper left corner. The movie was acquired and displayed at 10 frames/s. Scale bar, 5 μm.

Supplementary Movie 5. Related to Figure 2 and Supplementary Figure 2. Representative movie of KIX4 cell migration on VCAM-1-coated μ-channels under shear flow (3 dyn/cm^2). Fluorescence and DIC images over time (10 frames/s) are shown. Scale bar, 30 μm. Arrow in the movie indicates the direction of shear flow.

Supplementary Movie 6. Related to Figure 2 and Supplementary Figure 2. Representative movie of KIX4 cell migration on VCAM-1- and CXCL12-coated μ-channel under shear flow (3 dyn/cm^2). Fluorescence and DIC images over time (10

frames/s) are shown. Scale bar, 30 μm. Arrow in the movie indicates the direction of shear flow.

Supplementary Movie 7. Related to Figure 3 and Supplementary Figure 3. Representative movie showing migration of KIX4/FLNa_OsTIR1 control cells (DMSO-treated) in a VCAM-1- and CXCL12-coated μ-channel under shear flow (3 dyn/cm²). The movie displays time-lapse imaging in four panels: fluorescence at 488 nm (CXCR4-AcGFP, green), fluorescence at 561 nm (FLNa-mAID-mCherry2, red), merged fluorescence channels, and differential interference contrast (DIC). The movie was acquired at 10 frames/s. The arrow indicates the direction of the applied shear flow. Scale bar, 30 μm.

Supplementary Movie 8. Related to Figure 3 and Supplementary Figure 3. Representative movie showing migration of control KIX4/FLNa_OsTIR1 cells (DMSO-treated) in a VCAM-1-coated μ-channel under shear flow (3 dyn/cm²). The movie displays time-lapse fluorescence imaging in four panels: fluorescence at 488 nm (CXCR4-AcGFP), fluorescence at 561 nm (FLNa-mAID-mCherry2), merged fluorescence channels, and differential interference contrast (DIC). The movie was acquired at 10 frames/s. The arrow indicates the direction of the applied shear flow. Scale bar, 30 μm.

Supplementary Movie 9. Related to Figure 3 and Supplementary Figure 3. Representative movie showing migration of FLNa-deficient KIX4/FLNa_OsTIR1 cells (treated with DOX and auxin) in a VCAM-1-coated μ-channel under shear flow (3 dyn/cm²). The movie displays time-lapse fluorescence imaging in four panels: fluorescence at 488 nm (CXCR4-AcGFP), fluorescence at 561 nm (FLNa-mAID-mCherry2), merged fluorescence channels, and differential interference contrast (DIC). The movie was acquired at 10 frames/s. The arrow indicates the direction of the applied shear flow. Scale bar, 30 μm.

Supplementary Movie 10. Related to Figure 3 and Supplementary Figure 3. Representative movie showing migration of FLNa- deficient KIX4/FLNa_OsTIR1 cells (treated with DOX and auxin) in a VCAM-1- and CXCL12-coated μ-channel under shear flow (3 dyn/cm²). The movie displays time-lapse fluorescence imaging in four panels:

fluorescence at 488 nm (CXCR4-AcGFP, green), fluorescence at 561 nm (FLNa-mAID-mCherry2, red), merged fluorescence channels, and differential interference contrast (DIC). The movie was acquired at 10 frames/s. The arrow indicates the direction of the applied shear flow. Scale bar, 30 μm.

Supplementary Movie 11. Related to Figure 3. Representative movie showing migration of control KIX4/FLNa_OsTIR1 cells (DMSO-treated) in a VCAM-1-coated μ-channel under shear flow (3 dyn/cm²). The movie displays time-lapse imaging in two panels: interference reflection microscopy (IRM) and differential interference contrast (DIC). The movie was acquired at 10 frames/s. The arrow indicates the direction of the applied shear flow. Scale bar, 30 μm.

Supplementary Movie 12. Related to Figure 3. Representative movie showing migration of FLNa-deficient KIX4/FLNa_OsTIR1 cells (treated with DOX and auxin) in a VCAM-1-coated μ-channel under shear flow (3 dyn/cm²). The movie displays time-lapse imaging in two panels: interference reflection microscopy (IRM) and differential interference contrast (DIC). The movie was acquired at 10 frames/s. The arrow indicates the direction of the applied shear flow. Scale bar, 30 μm.

Supplementary Movie 13. Related to Figure 3. Representative movie showing migration of control KIX4/FLNa_OsTIR1 cells (DMSO-treated) in a VCAM-1- and CXCL12-coated μ-channel under shear flow (3 dyn/cm²). The movie displays time-lapse imaging in two panels: interference reflection microscopy (IRM) and differential interference contrast (DIC). The movie was acquired at 10 frames/s. The arrow indicates the direction of the applied shear flow. Scale bar, 30 μm.

Supplementary Movie 14. Related to Figure 3. Representative movie showing migration of FLNa-deficient KIX4/FLNa_OsTIR1 cells (treated with DOX and auxin) in a VCAM-1- and CXCL12-coated μ-channel under shear flow (3 dyn/cm²). The movie displays time-lapse imaging in two panels: interference reflection microscopy (IRM) and differential interference contrast (DIC). The movie was acquired at 10 frames/s. The arrow indicates the direction of the applied shear flow. Scale bar, 30 μm.

Supplementary Movie 15. Related to Figure 5B. 3D confocal reconstruction showing CXCR4-FLNa interactions detected by PLA (magenta dots) in human $CD4^+$ T lymphocytes migrating on VCAM-1-coated μ-channel at seven minutes. F-actin is shown in gray. Scale bar, 3μm.

Supplementary Movie 16. Related to Figure 5B. 3D confocal reconstruction showing CXCR4-FLNa interactions detected by PLA (magenta dots) in human $CD4^+$ T lymphocytes migrating on VCAM-1- and CXCL12-coated μ-channel at 7 minutes. F-actin is shown in gray. Scale bar, 3μm.

Supplementary Movie 17. Related to Figure 5B. 3D confocal reconstruction showing CXCR4-FLNa interactions detected by PLA (magenta dots) in human $CD4^+$ T lymphocytes migrating on VCAM-1- and CXCL12-coated μ-channel at 30 minutes. F-actin is shown in gray. Scale bar, 4μm.

Supplementary Movie 18. Related to Figure 5C-F. Representative movie of migrating KIX4 T cells transiently expressing mRuby-Rab4a, captured by dual-color SPT-TIRF microscopy. Cells were injected into μ-channels coated with VCAM-1 and CXCL12. The movie shows CXCR4-AcGFP (grayscale), mRuby-Rab4a (grayscale), and their merged fluorescence with CXCR4 in green and miRFP670_2-Rab4a in magenta. Only $CXCR4^+$/$Rab4^+$ endosomes are highlighted with white circles, and their trajectories are displayed in white in the merged movie. The movie was acquired at 20Hz and displayed at 10 frames/s. Scale bar, 5 μm.

Supplementary Movie 19. Related to Figure 5C-F. Representative movie of migrating FLNa-deficient KIX4 T cells (FLNaKOKIX4) transiently expressing mRuby-Rab4a, captured by dual-color SPT-TIRF microscopy. Cells were injected into μ-channels coated with VCAM-1 and CXCL12. The movie shows CXCR4-AcGFP (grayscale), mRuby-Rab4a (grayscale), and their merged fluorescence with CXCR4 in green and mRuby-Rab4a in magenta. Only $CXCR4^+$/$Rab4^+$ endosomes are highlighted with white circles, and their trajectories are displayed in white in the merged movie. The movie was acquired at 20Hz and displayed at 10 frames/s. Scale bar, 5 μm.

Supplementary Movie 20. Related to Figure 6. Representative movie of migrating KIX4 T cells transiently expressing miRFP670_2-Rab11a, captured by dual-color SPT-TIRF microscopy. Cells were injected into μ-channels coated with VCAM-1 and CXCL12. The movie shows CXCR4-AcGFP (grayscale), miRFP670_2-Rab11a (grayscale), and their merged fluorescence with CXCR4 in green and miRFP670_2-Rab11a in magenta. Only $CXCR4^+/Rab11^+$ endosomes are highlighted with white circles, and their trajectories are displayed in white in the merged movie. The movie was acquired at 20Hz and displayed at 10 frames/s. Scale bar, 5 μm.

Supplementary Movie 21. Related to Figure 6. Representative movie of migrating FLNa-deficient KIX4 T cells (FLNaKOKIX4) transiently expressing miRFP670_2-Rab11a, captured by dual-color SPT-TIRF microscopy. Cells were injected into μ-channels coated with VCAM-1 and CXCL12. The movie shows CXCR4-AcGFP (grayscale), miRFP670_2-Rab11a (grayscale), and their merged fluorescence with CXCR4 in green and miRFP670_2-Rab11a in magenta. Only $CXCR4^+/Rab11^+$ endosomes are highlighted with white circles, and their trajectories are displayed in white in the merged movie. The movie was acquired at 20Hz and displayed at 10 frames/s. Scale bar, 5 μm.

Supplementary Movie 22. Related to Figure 7 and Supplementary Figure 8. Representative movie showing migration of KIX4β1 cells in a VCAM-1-coated μ-channel under shear flow (3 dyn/cm²). The movie displays time-lapse imaging in four panels: fluorescence at 488 nm (CXCR4-AcGFP, green), fluorescence at 561 nm (β1 integrin-mCherry2, red), merged fluorescence channels, and differential interference contrast (DIC). The movie was acquired at 10 frames/s. The arrow indicates the direction of the applied shear flow. Scale bar, 30 μm.

Supplementary Movie 23. Related to Figure 7 and Supplementary Figure 8. Representative movie showing migration of KIX4β1 cells in a VCAM-1 and CXCL12-coated μ-channel under shear flow (3 dyn/cm²). The movie displays time-lapse imaging in four panels: fluorescence at 488 nm (CXCR4-AcGFP, green), fluorescence at 561 nm (β1 integrin-mCherry2, red), merged fuorescence channels, and differential interference

contrast (DIC). The movie was acquired at 10 frames/s. The arrow indicates the direction of the applied shear flow. Scale bar, 30 μm.

Supplementary Movie 24. Related to Figure 7. Representative movie of migrating KIX4β1 T cell captured by SPT-TIRF microscopy. Cells were injected into μ-channels coated with VCAM-1 under shear flow (3 dyn/cm²). The movie shows lateral diffusion of β1 integrin-mCherry2 spots during cell migration. The movie was acquired and displayed at 10 frames/s. Scale bar, 5 μm.

Supplementary Movie 25. Related to Figure 7. Representative movie of migrating KIX4β1 T cell captured by SPT-TIRF microscopy. Cells were injected into μ-channels coated with VCAM-1 and CXCL12 under shear flow (3 dyn/cm²). The movie shows lateral diffusion of β1 integrin-mCherry2 spots during cell migration. The movie was acquired and displayed at 10 frames/s. Scale bar, 5 μm.

Supplementary Movie 26. Related to Figure 7. Representative movie of migrating KIX4β1/FLNaKO T cell captured by SPT-TIRF microscopy. Cells were injected into μ-channels coated with VCAM-1 under shear flow (3 dyn/cm²). The movie shows lateral diffusion of β1 integrin-mCherry2 spots during cell migration. The movie was acquired and displayed at 10 frames/s. Scale bar, 5 μm.

Supplementary Movie 27. Related to Figure 7. Representative movie of migrating KIX4β1/FLNaKO T cell captured by SPT-TIRF microscopy. Cells were injected into μ-channels coated with VCAM-1 and CXCL12 under shear flow (3 dyn/cm²). The movie shows lateral diffusion of β1 integrin-mCherry2 spots during cell migration. The movie was acquired and displayed at 10 frames/s. Scale bar, 5 μm.

Supplementary Movie 28. Related to Supplementary Figure 10. Representative movie of migrating activated $CD4^+$ primary T lymphocyte infected with control LVPs $gp160_{IIIb}$-sh-Scramble (shScramble), stained with anti-β1 integrin antibody conjugated to AS635P (clone K20), and imaged by SPT-TIRF microscopy. Cells were injected into μ-channels coated with VCAM-1. The movie shows lateral diffusion of β1 integrin-AS635P spots

during cell migration under shear flow (3 dyn/cm²). The movie was acquired and displayed at 10 frames/s. Scale bar, 5 μm.

Supplementary Movie 29. Related to Supplementary Figure 10. Representative movie of migrating activated $CD4^+$ primary T lymphocyte infected with control LVPs $gp160_{IIIb}$-sh-Scramble (shScramble), stained with anti-β1 integrin antibody conjugated to AS635P (clone K20), and imaged by SPT-TIRF microscopy. Cells were injected into μ-channels coated with VCAM-1 and CXCL12. The movie shows lateral diffusion of β1 integrin-AS635P spots during cell migration under shear flow (3 dyn/cm²). The movie was acquired and displayed at 10 frames/s. Scale bar, 5 μm.

Supplementary Movie 30. Related to Supplementary Figure 10. Representative movie of migrating activated $CD4^+$ primary T lymphocyte infected with control LVPs $gp160_{IIIb}$-sh-FLNa (shFLNa), stained with anti-β1 integrin antibody conjugated to AS635P (clone K20), and imaged by SPT-TIRF microscopy. Cells were injected into μ-channels coated with VCAM-1. The movie shows lateral diffusion of β1 integrin-AS635P spots during cell migration under shear flow (3 dyn/cm²). The movie was acquired and displayed at 10 frames/s. Scale bar, 5 μm.

Supplementary Movie 30. Related to Supplementary Figure 10. Representative movie of migrating activated $CD4^+$ primary T lymphocyte infected with control LVPs $gp160_{IIIb}$-sh-FLNa (shFLNa), stained with anti-β1 integrin antibody conjugated to AS635P (clone K20), and imaged by SPT-TIRF microscopy. Cells were injected into μ-channels coated with VCAM-1 and CXCL12. The movie shows lateral diffusion of β1 integrin-AS635P spots during cell migration under shear flow (3 dyn/cm²). The movie was acquired and displayed at 10 frames/s. Scale bar, 5 μm.